Volume 52 | Number 42 | 25 May 2016 | Pages 6851–6948

ChemComm

Chemical Communications

www.rsc.org/chemcomm

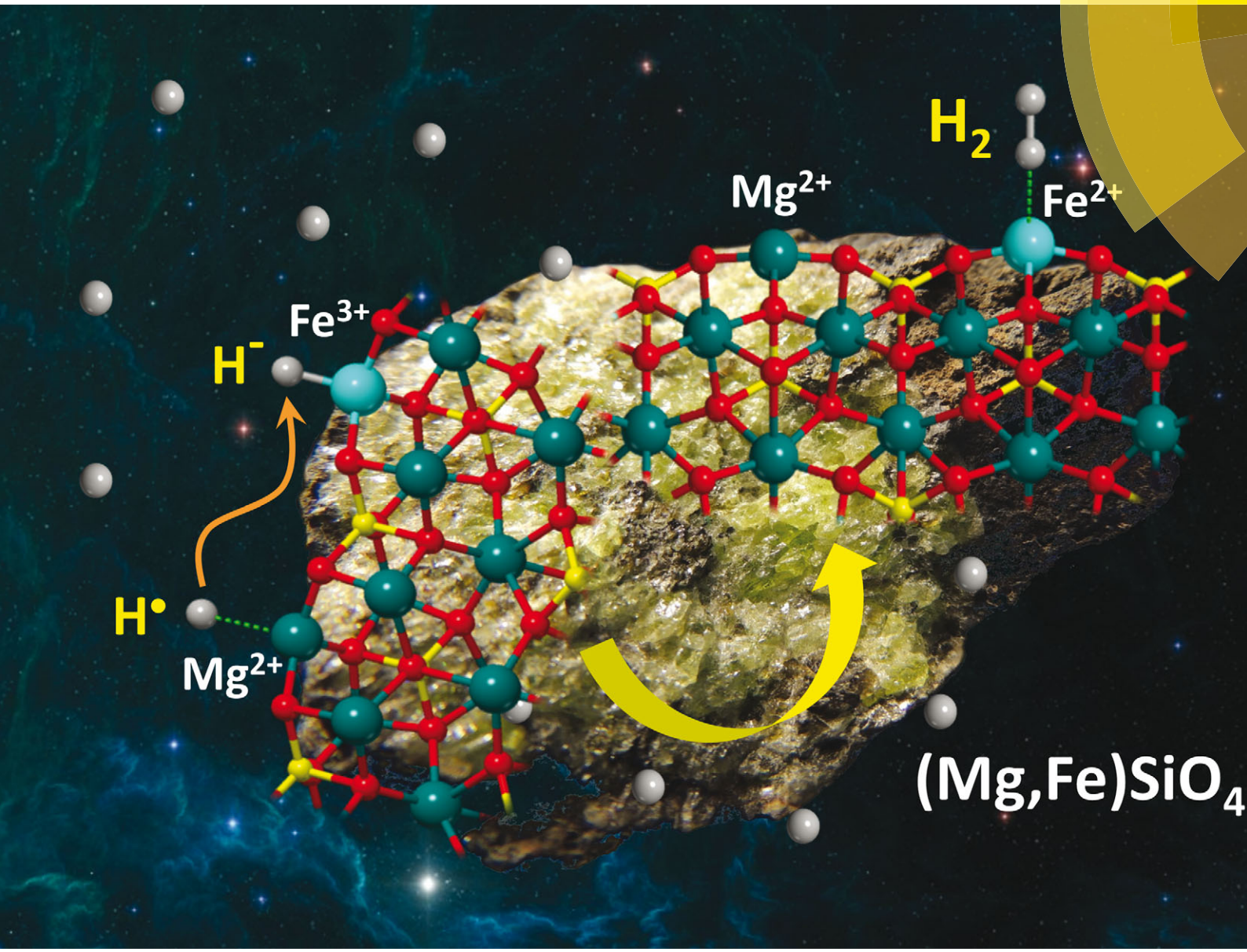

ISSN 1359-7345

ROYAL SOCIETY OF CHEMISTRY

COMMUNICATION

A. Rimola *et al.*

Does Fe^{2+} in olivine-based interstellar grains play any role in the formation of H_2? Atomistic insights from DFT periodic simulations

175 YEARS

ChemComm

COMMUNICATION

View Article Online
View Journal | View Issue

Cite this: *Chem. Commun.*, 2016, 52, 6873

Received 16th March 2016,
Accepted 14th April 2016

DOI: 10.1039/c6cc02313d

www.rsc.org/chemcomm

Does Fe^{2+} in olivine-based interstellar grains play any role in the formation of H_2? Atomistic insights from DFT periodic simulations†

J. Navarro-Ruiz,[a] P. Ugliengo,[b] M. Sodupe[a] and A. Rimola*[a]

Using periodic DFT-D2 methods, atomistic simulations of interstellar H adsorption and H_2 formation on a (010) Fe-containing olivine surface are presented. At variance with the (010) Mg_2SiO_4 surface and key to these processes are the large Fe/H interaction energies, suggesting that olivine surfaces are good reservoirs of H atoms for subsequent recombination to form H_2.

Understanding how H_2 is formed in the interstellar medium (ISM) is of fundamental relevance for several reasons.[1] Among the different molecular species detected, H_2 is the most abundant molecule and is observed in every ISM environment. From an astrophysical perspective, H_2 is an effective coolant of interstellar clouds during their gravitational collapse, thus facilitating the star formation, whereas from an astrochemical point of view, it plays a crucial role in most reaction networks to form other molecules, through neutral (H_2) and ionized (H_2^+ and H_3^+) forms.

It is well established that the conversion of atomic H into molecular H_2 requires the presence of interstellar dust grains (IDGs), sub-micron sized particles consisting of silicaceous and carbonaceous materials.[2] This is because the gas-phase radiative association of two ground state H atoms (*i.e.*, $H + H \rightarrow H_2 + h\nu$) has a very low rate coefficient ($\approx 10^{-29}$ cm^3 s^{-1})[3] due to spin forbidden transitions from the dissociative ($^3\Sigma_u^+$) to the ground electronic state ($^1\Sigma_g^+$). Several experimental reports[4–14] and astrochemical modelling studies[2,15] have shown that IDGs allow efficient H recombination to justify the large observed H_2 abundances. An excellent review on this subject was recently published by Vidali.[16]

Silicates, and in particular olivines and pyroxenes ($Mg_{2x}Fe_{(2x-2)}SiO_4$ and $Mg_xFe_{(x-1)}SiO_3$ (x = 0–1), respectively), are important constituents of IDGs. Several theoretical studies have addressed H adsorption and H_2 formation on silicate surfaces, using either cluster or periodic approaches to mimic the IDG surfaces, as well as using different DFT methods.[17–22] Nevertheless, practically all of them focused on Mg-pure silicates, with only one addressing the H adsorption on Fe_2SiO_4.[22] Fe^{2+} has a $3d^6$ electronic configuration that may lead to the formation of different low-lying electronic states and thus, it exhibits a more complex electronic structure than Mg^{2+}, leading to the inference of a more interesting chemistry towards H adsorption and, accordingly, towards its reactivity. In the following, we report the results of H adsorption and subsequent recombination to form H_2 on a Fe-containing olivine model surface, treated by *ab initio* periodic calculations performed using the CRYSTAL09 code,[23] with the main goal of assessing whether Fe^{2+} plays any significant and/or different role than Mg-pure olivines.

Crystalline silicates in IDGs are Fe-poor in composition (10–15% of the total metal content), whereas amorphous silicates are richer in Fe (up to ratios of Fe/Mg $\approx$ 1) but most of them either belong to the silicate matrix or are in the form of admixtures of metallic Fe.[24,25] Accordingly, the amount of Fe placed at the IDG surfaces is relatively small. In this work, we adopted a periodic surface model of (010) Mg_2SiO_4 by replacing one surface Mg^{2+} by Fe^{2+} per unit cell (see Fig. 1A), giving rise a surface with the formula $Mg_{1.875}Fe_{0.125}SiO_4$, hereafter referred to as Ol(010). The presence of only one surface Fe^{2+} cation will avoid us working with complex electronic configurations and, as Ol(010) has one Fe^{2+} and one Mg^{2+} at the outermost positions, it will help us to gain a better understanding of the role of Fe^{2+} and a proper comparison with Mg^{2+}.

In a previous work,[26] we have described that Fe^{2+} in its quintet state placed at the outermost positions of the (010) slab gives the most stable Fe-containing surfaces. Nonetheless, in the present work, the adsorption of one H atom on Fe^{2+} leads to change in the oxidation state, resulting in either a quartet or a sextet spin configuration. Therefore, we performed a previous calibration study comparing the energy difference between the sextet and quartet states calculated with different DFT methods and at the CCSD(T) level on a cluster model consisting of the first Fe coordination sphere (the ESI† shows the cluster model adopted). This calibration study was performed using the Gaussian09 code.[27]

[a] *Departament de Química, Universitat Autònoma de Barcelona, 08193 Bellaterra, Spain. E-mail: albert.rimola@uab.cat*
[b] *Dipartimento di Chimica and NIS – Nanostructured Interfaces and Surfaces – Interdepartment Centre, Università degli Studi di Torino, Via P. Giuria 7, 10125 Torino, Italy*

† Electronic supplementary information (ESI) available: Energetic values and structures, and extended computational details. See DOI: 10.1039/c6cc02313d

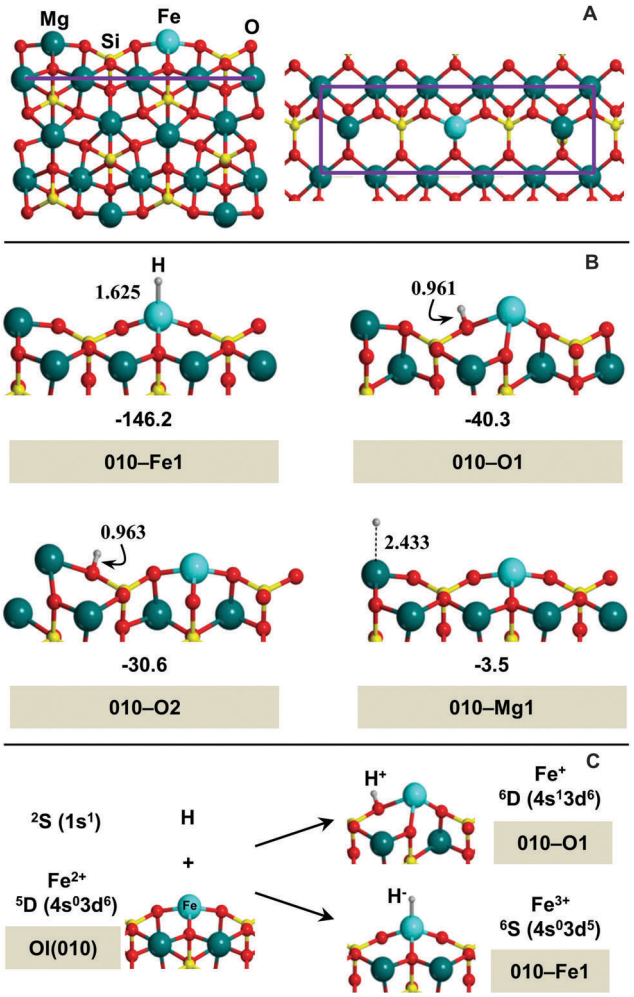

Fig. 1 (A) Lateral and top views of the Fe-containing olivine surface model used in this work. Details can be found in ref. 26. Unit cell is highlighted in purple. (B) BHLYP-D2*//BHLYP-optimized geometries of the different complexes for the H adsorption on the Fe-containing surface at the sextet state. Bond distances (in Å) and adsorption energies including zero-point energy corrections (in kJ mol^{-1}) are also included. (C) Scheme of the electronic reorganization occurring in the 010-O1 and 010-Fe1 adducts.

At CCSD(T), the sextet state is more stable than the quartet state by 71.3 kJ mol^{-1}. GGA DFT methods and hybrid methods with a low exact exchange percentage underestimate this energy difference (between 0.4 and 55.5 kJ mol^{-1}), whereas methods with a large amount of exact exchange give much better agreement (between 78.5 and 99.5 kJ mol^{-1}). This is because the inclusion of an exact exchange tends to stabilize high-spin states.[28] The hybrid BHLYP functional, implemented in CRYSTAL, performs reasonably well (energy difference of 88.5 kJ mol^{-1}), so that it was the method of choice for all calculations. As we adopted B3LYP-D2* in previous studies[20,21] (namely, geometry optimization at the B3LYP level combined with a reparametrized D2 correction term[29,30] for dispersion), we also repeated the calculations at this level for the sake of comparison, which are included in the ESI.† It is worth mentioning that the second ionization energies for Mg and Fe calculated at BHLYP are in excellent agreement with those calculated at CCSD(T) and with the experimental values, whereas B3LYP provides overestimated values (data reported in the ESI†). To take dispersion into account at the BHLYP level, the D2* values obtained at B3LYP-D2* were introduced to the energies of the BHLYP-optimized geometries (hereafter referred to as BHLYP-D2*//BHLYP energies). We optimized the structures with a polarized double-ζ basis set and improved the energies through single-point calculations with the polarized triple-ζ basis set on the optimized geometries. See the ESI† for further computational details and calibration calculations.

The adsorption of one H atom on Ol(010) gave four possible adducts in the sextet state (shown in Fig. 1B) in which the H atom interacts with (i) the Fe atom (010-Fe1), (ii) the uppermost Mg atom (010-Mg1), (iii) the O atom closer to Fe (010-O1), and (iv) the O atom closer to Mg (010-O2). 010-Mg1 is a physisorption state as shown by the spin densities (+0.96/+3.90 on H/Fe) and the Mg–H distance (2.433 Å). All the remaining adducts are chemisorbed states as shown by (i) the spin density on H, which is almost null, (ii) the typical O–H distances (~0.96 Å) in 010-O1 and 010-O2, and (iii) the Fe–H distance of 1.625 Å in 010-Fe1. In 010-O2, the spin density of H is transferred to the closest Mg^{2+} ion (spin density of Mg varies from 0.0 to +0.95), thus the metal cation exhibiting a partial reduction and the H atom acquiring a certain H^+ character (charge of +0.33|*e*|) in agreement with the SiOH stoichiometry. Similar phenomena occur in 010-O1; *i.e.*, upon H adsorption, the spin density is transferred to the Fe^{2+} ion (spin density of Fe varies from +3.90 to +4.93), which becomes partially reduced. Moreover, the spin state of Fe implies five unpaired electrons in a ^{6}D ($4s^13d^6$) electronic configuration, which is the most stable electronic state of a naked Fe^+ ion. In 010-Fe1, the charge of the H atom is −0.26|*e*|, implying a certain H^- character. In this adduct, Fe is partially oxidized, and the metal spin density varies from +3.90 to +4.58, which leads to an electronic configuration close to that of Fe^{3+} ($3d^5$). Fig. 1C summarizes the electronic reorganization described above by the 010-O1 and 010-Fe1 adducts. Fig. 1B shows the calculated adsorption energies of these complexes, whose trend is (from more to less stable) as follows: 010-Fe1 ≫ 010-O1 > 010-O2 ≫ 010-Mg1. In summary, the chemisorption of H at the Fe site on Ol(010) leads to a strong Fe–H bond. This is at variance with the H adsorption on the (010) Mg_2SiO_4 surface,[20] in which physisorption occurs on Mg atoms and weak chemisorption on O atoms. Interestingly, H diffusion adopting the 010-Mg1 → 010-O2 → 010-O1 → 010-Fe1 path has been calculated providing energy barriers of 30, 166 and 83 kJ mol^{-1}, respectively (see the ESI†). Since H adsorption on Fe is barrierless, the jump from 010-Mg1 to 010-Fe1 is expected to occur through H desorption–adsorption steps, similarly to what was found in forsterite surfaces.[20,21]

To simulate the formation of H_2 on Ol(010), we started by adsorbing a second H atom on the singly-H adsorbed systems described above. Eight adsorbed complexes resulted in both the quintet and the heptet state, with the former state being the most stable one (see the ESI† for structural and energetic data of these systems). Moreover, since the quintet state is the one that will lead to H_2 formation, from now on we will present only the results for this spin state. It should be noted that for all systems involving the adsorption of two H atoms we adopted an

open shell broken symmetry as a starting guess. According to our previous experience,[20,21] only three of them are suitable reactants for the H_2 formation as shown in Fig. 2A. The 010-Fe1–Mg1 structure is the least stable one, due to one physisorbed H atom at the surface Mg, while the major contribution to the adsorption energy is due to the strong Fe–H bond. The most stable complexes (010-O2–Mg1 and 010-Fe1–O1) both show chemisorption with respect to the two H ad-atoms, at either Mg or Fe ions and at neighbouring O atoms. The most stable precursor species for 010-O2–Mg1 is the 010-O2 complex. In 010-O2, the unpaired electron was fully on the Mg atom (see above), which upon second H adsorption couples with the H atom to give the Mg–H bond present in 010-O2–Mg1. The most stable precursor species of 010-Fe1–O1 is 010-Fe1. In this complex, the Fe ion is partially oxidized (see above). When the second H atom adsorbs on the Fe-neighbouring O atom, the transfer of electron charge reduces the Fe ion to its initial oxidation state. Therefore, the high stability of 010-O2–Mg1 and 010-Fe1–O1 systems is due to the formation of both hydride (Mg–H or Fe–H) and Si–OH groups.

The recombination of the two H ad-atoms in 010-Fe1–Mg1 involves a radical–hydride reaction (Fig. 2A). The calculated energetics indicate a very low energy barrier (3.4 kJ mol^{-1}) followed by a large drop of the reaction energy due to H_2 formation (−277 kJ mol^{-1}). H recombination in both 010-O2–Mg1 and 010-Fe1–O1 is driven by a $H^{+}\cdots H^{-}$ coupling, with generally higher energy barriers (18.3 and 37.8 kJ mol^{-1}, respectively) compared to the radical–hydride coupling. This is due to the SiO–H and Mg–H/Fe–H bond breaking. The higher energy barrier in 010-Fe1–O1 than that in 010-O2–Mg1 is due to the stronger Fe–H bond than the Mg–H one. These two complexes are more stable than 010-Fe1–Mg1 so that the reaction energies are less negative (−80 and −62 kJ mol^{-1}, respectively). Once formed, H_2 remains adsorbed on the Ol(010) surface at the Mg or Fe ions (see structures of 010-Mg1–H_2 and 010-Fe1–H_2 in Fig. 2A), with adsorption energies of −14.7 and −7.3 kJ mol^{-1}, respectively (see the ESI† for full details).

Kinetic chemical trends related to H_2 formation cannot be limited to the classical Eyring rate constant k^{TST}, as low T and the light H atom bring the quantum tunnel into play. Therefore, we calculated the tunnelling crossover temperatures (T_x)[31] (*i.e.*, the temperature below which tunnelling becomes dominant) and the rate constants using a semi-classical approach ($k^{SC\text{-}TST}$), in which tunnelling is accounted for by correcting the k^{TST} with the transmission coefficient $\Gamma(T)$, as suggested by Fermann and Auerbach.[31] With these values we built the Arrhenius plots (shown in Fig. 2B), in which $\Gamma(T)$ = 1.0 for T above T_x (see the ESI† for further details). In principle, the $\Gamma(T)$ formula is stable at arbitrarily low temperatures. Nonetheless, we considered $T > 150$ K, because lower T values require more accurate treatment for the tunnelling than the present one, like those adopted to study H adsorption on carbonaceous surfaces.[32,33] The Arrhenius plots for H_2 formation indicate that the tunnel does not contribute (no slope change) to the reaction involving the physisorbed H atom (*i.e.*, 010-Fe1–Mg1 → 010-Fe1–H_2). In contrast, reactions involving chemisorbed H atoms (*i.e.*, 010-O2–Mg1 → 010-Mg1–H_2 and 010-Fe1–O1 → 010-Fe1–H_2) do show a slope change revealing a crucial role of tunnelling for their occurrence. When performing linear extrapolations of the lines of the Arrhenius plots below T_x (*i.e.*, where tunnelling is important), the $\log_{10} k^{SC\text{-}TST}$ values extrapolated at 50 K are 7.3 and 4.1 for the 010-O2–Mg1 and 010-Fe1–O1, respectively, to be compared with the −12.7 and −34.8 values computed in the absence of tunnelling.

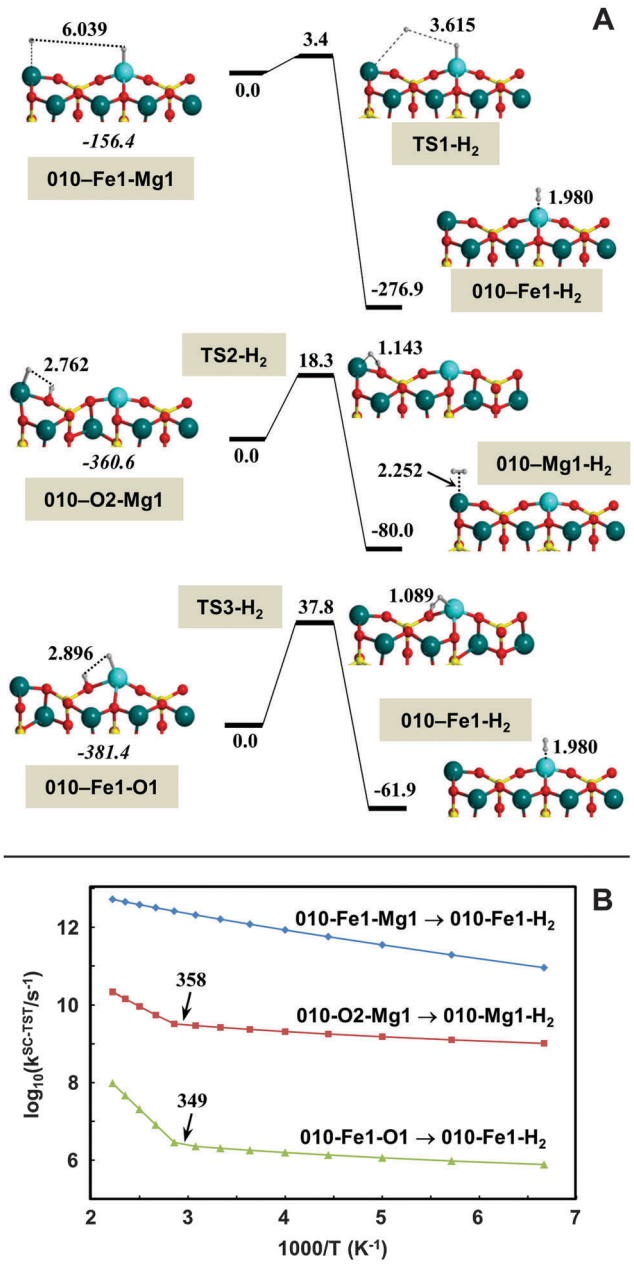

Fig. 2 (A) BHLYP-D2*//BHLYP-energy profiles including zero-point energy corrections (in kJ mol^{-1}) for H_2 formation from the most significant doubly-H adsorption complexes. All the structures are calculated in the quintet state, which are more stable than the heptet state (see the ESI†). Adsorption energies (values in italics above the reactants) are referenced with respect to the Ol(010) + 2H zero-energy asymptote, whereas values of the energy profiles are referenced with respect to the corresponding reactants. Bond distances are in Å. (B) Arrhenius plots of $k^{SC\text{-}TST}$ between 150 and 450 K for the H_2 formation processes using data calculated at BHLYP-D2*//BHLYP. Crossover temperatures (T_X, in K) are also indicated.

In our previous work,[20] we suggested that H_2 formation on the (010) Mg_2SiO_4 surface occurred when the H atoms physisorbed on two different Mg atoms recombine quickly through a radical–radical coupling, without tunnelling contributions. Moreover, it was shown that the tunnel was important to facilitate a proton–hydride coupling between H atoms chemisorbed on Mg/O ions in close spatial proximity. This effect is also operative on Ol(010) as shown by the similar process occurring from the 010-O2–Mg1 complex. Additionally, on Ol(010) there are two additional channels for H_2 formation envisaging a Fe–H bond. One channel occurs through a radical–hydride coupling between one H atom physisorbed on Mg and the other H atom chemisorbed on Fe (*i.e.*, from 010-Fe1–Mg1) with a very low barrier and without the contribution of tunnelling. The other channel takes place through a proton–hydride coupling between one H atom attached on O and the other bound to the neighbouring Fe ion (*i.e.*, from 010-Fe1–O1), in which tunnelling is advocated for its occurrence. In both cases reactions are calculated to be fast.

To sum up, the results of the present work indicate that Fe^{2+} cations do indeed play a role in the formation of the H_2 molecule in the ISM. H adsorption on Fe sites is much stronger than on Mg ones, due to favourable spin coupling. On Fe, H is chemisorbed in the form of hydride, whereas on Mg, H is mainly physisorbed, keeping its radical character. This indicates that Fe-containing olivines, due to the strong Fe–H bond, can capture H atoms for a very long time on an astronomical scale, an aspect of paramount importance considering the very low atomic densities of the ISM. Moreover, the capability of the (010) Fe-containing olivine surfaces to form H_2 *via* H recombination is kinetically comparable to the (010) Mg_2SiO_4 surface.

Financial support from MICINN (CTQ2014-59544-P, CTQ2014-60119-P and CTQ2015-62635-ERC) and DIUE (project 2014SGR482) is gratefully acknowledged. JN-R is indebted to SUR of ECO of Generalitat de Catalunya for a predoctoral grant. AR is indebted to Programa Banco de Santander for a UAB distinguished postdoctoral research contract. MS gratefully acknowledges support through the 2011 ICREA Award. PU acknowledges Progetti di Ricerca di Ateneo-Compagnia di San Paolo-2011-Linea 1A, progetto ORTO11RRT5 for funding. AR kindly acknowledges BSC-MN for the generous allowance of computing time through the 'QCM-2013-2-0006: Formation of Molecular Hydrogen on Surfaces of Cosmic Dust', 'QCM-2013-3-0015: Adsorption of Atomic Hydrogen on Defective Non-Stoichiometric Surfaces of Cosmic Dust' and 'QCM-2014-3-0032: Quantum Effects in the Diffusion of Atomic Hydrogen on Interstellar Silicate Surfaces' projects. The use of the Catalonia Supercomputer Centre (CESCA) is gratefully acknowledged.

Notes and references

1 J. E. Dyson and D. A. Williams, *The Physics of the Interstellar Medium*, Taylor & Francis, New York, 2nd edn, 1997.
2 R. J. Gould and E. E. Salpeter, *Astrophys. J.*, 1963, **138**, 393–407.
3 W. W. Duley and D. A. Williams, *Interstellar Chemistry*, Academic Press, Orlando, 1984.
4 L. Hornekær, A. Baurichter, V. V. Petrunin, D. Field and A. C. Luntz, *Science*, 2003, **302**, 1943–1946.
5 L. Hornekær, Ž. Šljivančanin, W. Xu, R. Otero, E. Rauls, I. Stensgaard, E. Lægsgaard, B. Hammer and F. Besenbacher, *Phys. Rev. Lett.*, 2006, **96**, 156104.
6 H. B. Perets, O. Biham, G. Manicó, V. Pirronello, J. Roser, S. Swords and G. Vidali, *Astrophys. J.*, 2005, **627**, 850.
7 H. B. Perets, A. Lederhendler, O. Biham, G. Vidali, L. Li, S. Swords, E. Congiu, J. Roser, G. Manicó, J. R. Brucato and V. Pirronello, *Astrophys. J., Lett.*, 2007, **661**, L163.
8 G. Vidali, J. E. Roser, L. Ling, E. Congiu, G. Manico and V. Pirronello, *Faraday Discuss.*, 2006, **133**, 125–135.
9 S. Baouche, G. Gamborg, V. V. Petrunin, A. C. Luntz, A. Baurichter and L. Hornekær, *J. Chem. Phys.*, 2006, **125**, 084712.
10 S. C. Creighan, J. S. A. Perry and S. D. Price, *J. Chem. Phys.*, 2006, **124**, 114701.
11 F. Islam, E. R. Latimer and S. D. Price, *J. Chem. Phys.*, 2007, **127**, 064701.
12 N. Katz, I. Furman, O. Biham, V. Pirronello and G. Vidali, *Astrophys. J.*, 1999, **522**, 305.
13 V. Pirronello, O. Biham, C. Liu, L. Shen and G. Vidali, *Astrophys. J., Lett.*, 1997, **483**, L131.
14 J. He, P. Frank and G. Vidali, *Phys. Chem. Chem. Phys.*, 2011, **13**, 15803–15809.
15 S. Cazaux and A. G. G. M. Tielens, *Astrophys. J.*, 2004, **604**, 222–237.
16 G. Vidali, *Chem. Rev.*, 2013, **113**, 8762–8782.
17 S. Garcia-Gil, D. Teillet-Billy, N. Rougeau and V. Sidis, *J. Phys. Chem. C*, 2013, **117**, 12612–12621.
18 T. P. M. Goumans, C. R. A. Catlow and W. A. Brown, *Mon. Not. R. Astron. Soc.*, 2009, **393**, 1403–1407.
19 B. Kerkeni and S. T. Bromley, *Mon. Not. R. Astron. Soc.*, 2013, **435**, 1486–1492.
20 J. Navarro-Ruiz, M. Sodupe, P. Ugliengo and A. Rimola, *Phys. Chem. Chem. Phys.*, 2014, **16**, 17447–17457.
21 J. Navarro-Ruiz, J. Á. Martínez-González, M. Sodupe, P. Ugliengo and A. Rimola, *Mon. Not. R. Astron. Soc.*, 2015, **453**, 914–924.
22 C. A. Downing, B. Ahmady, C. R. A. Catlow and N. H. de Leeuw, *Philos. Trans. R. Soc., A*, 2013, **371**, 20110592.
23 R. Dovesi, V. R. Saunders, C. Roetti, R. Orlando, C. M. Zicovich-Wilson, F. Pascale, B. Civalleri, K. Doll, N. M. Harrison, I. J. Bush, P. D'Arco and M. Llunell, *CRYSTAL09 User's Manual*, University of Torino, Torino, 2009.
24 T. Henning, *Annu. Rev. Astron. Astrophys.*, 2010, **48**, 21–46.
25 F. Molster and C. Kemper, *Space Sci. Rev.*, 2005, **119**, 3–28.
26 J. Navarro-Ruiz, P. Ugliengo, A. Rimola and M. Sodupe, *J. Phys. Chem. A*, 2014, **118**, 5866–5875.
27 M. J. Frisch, *et al.*, *Gaussian 09*, Wallingford CT, 2013.
28 M. Reiher, O. Salomon and B. Artur Hess, *Theor. Chem. Acc.*, 2001, **107**, 48–55.
29 S. Grimme, *J. Comput. Chem.*, 2006, **27**, 1787–1799.
30 B. Civalleri, C. M. Zicovich-Wilson, L. Valenzano and P. Ugliengo, *CrystEngComm*, 2008, **10**, 405–410.
31 J. T. Fermann and S. Auerbach, *J. Chem. Phys.*, 2000, **112**, 6787–6794.
32 T. P. M. Goumans, *Mon. Not. R. Astron. Soc.*, 2011, **415**, 3129–3134.
33 T. P. M. Goumans and J. Kästner, *Angew. Chem., Int. Ed.*, 2010, **49**, 7350–7352.

